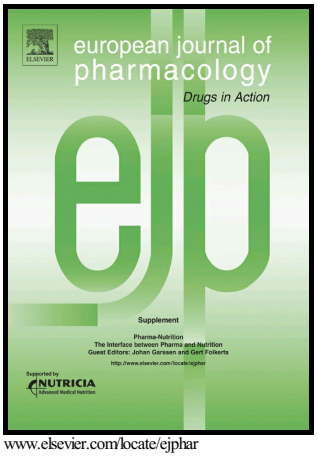

www.elsevier.com/locate/ejphar

Deoxynucleosides with benzimidazoles as aglycone moiety are potent anticancer agents

Mirosława Koronkiewicz, Zdzisław Chilmonczyk, Zygmunt Kazimerczuk, Andrzej Orzeszko

PII: S0014-2999(17)30809-9
DOI: https://doi.org/10.1016/j.ejphar.2017.12.018
Reference: EJP71565

To appear in: *European Journal of Pharmacology*

Received date: 16 October 2017
Revised date: 1 December 2017
Accepted date: 8 December 2017

Cite this article as: Mirosława Koronkiewicz, Zdzisław Chilmonczyk, Zygmunt Kazimerczuk and Andrzej Orzeszko, Deoxynucleosides with benzimidazoles as aglycone moiety are potent anticancer agents, *European Journal of Pharmacology,* https://doi.org/10.1016/j.ejphar.2017.12.018

Deoxynucleosides with benzimidazoles as aglycone moiety are potent anticancer agents

Mirosława Koronkiewicz[a], Zdzisław Chilmonczyk[a],

Zygmunt Kazimerczuk[b], Andrzej Orzeszko[b]

[a]*Department of Cell Biology, National Medicines Institute, Chełmska St. 30/34, 00-725 Warsaw, Poland*

[b]*Institute of Chemistry, Warsaw University of Life Sciences, Nowoursynowska St. 159C, 02-787 Warsaw, Poland*

Correspondence to: Mirosława Koronkiewicz, Department of Cell Biology, National Medicines Institute, Chełmska St. 30/34, 00-725 Warsaw, Poland, Tel.: + 4822 851 43 79, Fax: + 4822 841 06 52, e-mail: m.koronkiewicz@nil.gov.pl

[1]Abstract. Abnormally high levels of CK2 and PIM-1 serine/threonine kinases have been documented in many cases of cancer. The elevation of CK2 and PIM-1 in cells entails suppression of apoptosis and implies a protective role for the kinases against cell death. Downregulation of these enzymes by chemical methods promotes apoptosis in cells. The aim of the present study was to explore the anticancer activity of inhibitors of protein kinases CK2 and PIM-1 on neoplastic cell lines *in vitro.* We studied a series of deoxynucleosides with various tetrahalobenzimidazoles as aglycone moiety. Cytotoxicity, induction of apoptosis by the tested inhibitors, mitochondrial membrane potential, activity of caspases, changes in cell cycle progression, as well as a mechanism of action were determined by flow cytometry and other methods. The results indicate that the studied compounds, *e.g.*, 1-(β-D-2′-deoxyribofuranosyl)-4,5,6,7-tetrabromo-1*H*-benzimidazole called K164 (also termed TDB), showed diverse cytotoxicity and proapoptotic efficacy in cell lines. Our results showed that the tested compounds are potential anticancer agents for targeted therapy, particularly in the treatment of myeloid leukaemia and androgen-responsive prostate cancer.

Key Words: Protein kinase inhibitors, tetrahalobenzimidazoles, anticancer effects, flow cytometry

[1] Preliminary results were presented as a poster at the EMBO conference series. Cellular Signaling & Cancer Therapy. May 27-31, 2016 | Cavtat-Dubrovnik, Croatia. Abstract was published in the Abstracts of poster presentations.

1. Introduction

Constitutively active serine/threonine kinases such as CK2 (casein kinase 2) and the PIMs family (Proviral Integration site of Moloney Virus) with special reference to PIM-1 show abnormally high levels in a number of cancers and mediate important hallmarks of cancer, particularly suppression of apoptosis (Ahmed et al., 2008; Pinna, 2012; Brault et al., 2010; Nawijn et al., 2011; Amaravadi et al., 2005). Overexpression of kinases CK2 and PIM-1 in patient tumours frequently correlates with poor prognosis and is considered an unfavourable prognostic marker in prostate and lung cancers, acute myeloid leukaemia, and pancreatic ductal adenocarcinoma (O-charoenrat at al., 2004; Kim et al., 2007; Laramas et al., 2007; Dhanasekaran et al., 2001; Cibull et al., 2006; Reiser-Erkan et.al., 2008). Downregulation of these kinases by chemical methods was found to promote apoptosis in cells and targeted CK2 and PIM-1 for cancer therapy (Koronkiewicz et al., 2010, 2013; Wang et al., 2008; Kaminska at al. 2009; Trembley at al. 2010; Duncan at al. 2013).

A number of highly specific heterocyclic compounds have been developed to target CK2 including 4,5,6,7-tetrabromo-1*H*-benzotriazole (TBB also termed TBBt) (Sarno et al. 2001; Bretner et al. 2008) 4,5,6,7-tetrabromo-1*H*-benzimidazole (TBI also termed TBBz), 2-dimethylamino-4,5,6,7-tetrabromo-1*H*-benzimidazole (DMAT) (Pagano et al. 2004; Zien et al. 2003), as well as novel tetrahalogenated benzimidazoles (Gianoncelli et al. 2009; Janeczko et al. 2012; Schneider et al. 2012). The first orally available small molecule inhibitor of CK2 protein in clinical trials for cancer was CX-4945 (Cylene Pharmaceuticals, San Diego, CA, USA) (Siddiqui-Jain et al. 2010). ATP-competitive small-molecule inhibitors of the PIM1 kinase with growth inhibitory activity against leukaemia and prostate cancer cells have also been reported (Pogacic et al. 2007; Fedorov et al. 2007). Quercetagetin has been recognized to be a moderately potent and selective cell permeable inhibitor of PIM-1 kinase that is able to inhibit PIM-1 activity in prostate cancer cells in a dose-dependent fashion (Holder et al.

2007). SGI-1776 (Astex) was found to be a potent adenosine-5'-triphosphate (ATP) competitive inhibitor of Pim-1, Pim-2, and Pim-3 kinases with half maximal inhibitory concentrations of 7 nM, 363 nM and 69 nM, respectively (Chen et al. 2009; Cervantes-Gomez et al. 2013), and a novel series of meridianin C derivatives substituted at C-5 position was prepared (More et al. 2014).

Previous research has shown that the majority of tetrahalogenated benzimidazoles, particularly tetrabromo- and tetraiodobenzimidazoles, showed strong activity as inhibitors of CK2, PIM-1, DYRK1A and other kinases, such as Rio1 (Kubiński et al. 2017), *in vitro*. Unfortunately, these compounds are not cell permeable and thus cannot be used for medical purposes. To avoid this fault, selective powerful cell-permeable dual inhibitors of protein kinases CK2 and PIM-1 were synthesized (Lopez-Ramos et al. 2010; Pagano et al. 2008; Cozza et al. 2013, 2014; Girardi et al. 2015). The addition of a sugar moiety (deoxyribose) to halogenobenzimidazole molecules *via* C-N bonds improves their solubility and provides effective intercellular transport (Cozza et al. 2013). Among the compounds synthesized, 1-(β-D-2′-deoxyribofuranosyl)-4,5,6,7-tetrabromo-1*H*-benzimidazole, called K164 (also termed TDB), seems to be the most promising. 1`Cozza G. and co-authors demonstrated that the cytotoxic efficacy of TDB is almost entirely due to apoptosis, is accompanied by parallel inhibition of cellular CK2 and PIM-1 and is superior to that observed either by combining individual inhibitors of CK2 and PIM-1 or by treating cells with the CK2 inhibitor CX4945 (Cozza et al. 2014). Comparing the persistence of CK2 inhibition after their administration to cells showed that the effect of TDB on CK2 activity is more long-lasting than that of CX-4945, with important consequences for cellular processes affected by CK2 such as cell survival, proliferation and migration (Cozza et al. 2015).

In our previous publications we presented that many substituted tetrahalobenzimidazoles (e.g., 4,5,6,7-tetraiodo-1*H*-benzimidazole; 4,5,6,7-tetrabromo-1*H*-benzimidazole; 4,5,6,7-

tetrabromo-2-(4-methylpiperazin-1-yl)-1*H*-benzimidazole; 4,5,6,7-tetrabromo-2-(4-methyl-piperazin-1-yl)-1*H*-benzimidazole; 2-aminoethyleneamino-4,5,6,7-tetrabromo-1*H*-benzimi-dazole) not only inhibited isolated kinases but also showed, in some cases, activity against prostate cancer and leukaemia cell lines (HL-60, KG-1, LNCaP) (Koronkiewicz et al. 2010, 2013; Schneider et al. 2012). These interesting findings, particularly for TDB (Cozza et al. 2013, 2014; Girardi et al. 2015), encouraged us to continue and extend our investigations. In the present study, we reported the anticancer activity of TDB (K164) and its five analogues against leukaemia and prostate cell lines *in vitro.* We examined the activity of the compounds against two leukaemia (KG-1, human acute myelogenous leukaemia and K562, human chronic erythromyeloblastoid leukaemia) and two prostate (PC-3, androgen-independent human prostate adenocarcinoma and LNCaP, androgen-responsive human prostate adenocarcinoma) cell lines. It should be noted that the pro-apoptotic activity of the very same compounds was recently examined on human T lymphoblastoid (CEM) and its multi-drug resistance variant (R-CEM), human cervical cancer (HeLa), human embryonic kidney (HEK-293T) cells and CCD34Lu human neonatal lung fibroblasts (CCd34Lu) (Cozza et al. 2014).

2. Materials and methods

2.1. Chemistry

All nucleosides (1-6) were synthesized using the same procedure as described previously (Cozza et al. 2013, 2014). Analytical data for these compounds have also been published in cited publications. In this paper, we recall the general method of synthesis, as well as the data for 1, as an example. The synthesis scheme and chemical structure of the studied compounds are shown in Fig. 1.

2.1.1. General procedure for preparation of inhibitors 1-6

To a suspension of proper benzimidazole (4 mmol) in dry acetonitrile (70 ml), sodium hydride (200 mg, 5 mmol, 60% in oil) was added portion-wise. The mixture was stirred and refluxed for 10 min. After cooling, 2-deoxy-3,5-bis-*O*-(4-methylbenzoyl)-β-D-*erythro*-pentafuranosyl chloride (4 mmol) was added in portions. The mixture was stirred for 20 min at room temperature. Then, methylene chloride (70 ml) was added and the mixture filtered through Cellite. The solvent was evaporated and the residue was chromatographed on a silica gel column with toluene-acetone (95:5, v/v) as an eluent. The fractions containing the main product were evaporated, and the residue crystallized from methanol to give white needles.

By way of example analytical data for 1-[2-deoxy-3,5-di-*O*-(4-methylbenzoyl)-β-D-*erythro*-pentofuranosyl]-4,5,6,7-tetrachlorobenzimidazole are shown: Yield: (1.09 g, 45%); mp 191-192 °C; ^{1}H NMR (DMSO-d_6): δ 2.37 (s, 3H), 2.40 (s, 3H), 2.96 (m, 1H), 3.07 (m, 1H), 4.52 (m, 2H), 4.58 (m, 1H), 5.72 (m, 1H), 7.01 (t, *J* = 6.4 Hz, 1H), 7.30-8.0 (4d, arom. H, 8H), 8.82 (s, 1H). *Anal*. Calcd. for $C_{28}H_{22}Cl_4N_2O_5$ (608.31): C, 55.29; H, 3.65; N, 4.61. Found: C, 55.25; H, 3.60; N, 4.52 (Cozza et al. 2013).

2.1.2. 1-(2-Deoxy-β-D-erythro-pentofuranosyl)-4,5,6,7-tetrachlorobenzimidazole (1). A mixture of 1-[2-deoxy-3,5-di-*O*-(4-methylbenzoyl)-β-D-*erythro*-pentofuranosyl] (2.63 mmol) and methanolic sodium methanolate (50 ml, 0.1 M) was stirred and refluxed for 15 min. Methanol was evaporated, and the residue purified by flash chromatography on silica gel using chloroform as an eluent. The fractions containing product were evaporated, and the residue crystallized from methanol water to give colourless needles. Yield: (685 mg, 70%), mp 141-144 °C; ^{1}H NMR (DMSO-d_6): δ 2.46 (m, 1H), 2.58 (m, 1H), 3.65 (2m, 2H), 3.89 (q, *J* = 3.9 Hz, 1H), 4.47 (m, 1H), 5.04 (t, *J* = 5.2 Hz, 1H), 5.36 (d, *J* = 4.5 Hz, 1H), 6.85 (t, *J* = 5.9 Hz, 1H), 8.88 (s, 1H). uv (MeOH): λ (ε) 225 (22 400). 270 (9 200), 298 (3 100). *Anal*. Calcd.

for $C_{12}H_{10}Cl_4N_2O_3$ (372.04): C, 38.74; H, 2.71; N, 7.53. Found: C, 38.66; H, 2.77; N, 7.47 (Cozza et al. 2013).

2.2. Cell culture and treatment with agents

The following cell lines were used in this study: KG-1 (human acute myelogenous leukaemia), K562 (human chronic erythromyeloblastoid leukaemia), PC-3 (androgen-independent human prostate adenocarcinoma) and LNCaP (androgen-responsive human prostate adenocarcinoma). Cell lines were purchased from the American Type Culture Collection (ATCC, Manassas, VA, USA).

KG-1 cells were grown in IMDM medium (CytoGen, Sinn, Germany) supplemented with 20% (v/v) heat-inactivated foetal bovine serum (CytoGen), 1% (v/v) antibiotic–antimycotic solution (CytoGen) and 1% (v/v) stable glutamine (L-alanyl-L-glutamine) solution (CytoGen). K562 and PC-3 cell lines were cultured in RPMI 1640 (CytoGen) supplemented with 10% (v/v) heat-inactivated foetal bovine serum (CytoGen), 1% (v/v) antibiotic–antimycotic solution (CytoGen) and 1% (v/v) stable glutamine (L-alanyl-L-glutamine) solution (CytoGen). LNCaP cell line was cultured in RPMI 1640 (CytoGen) supplemented with 10% (v/v) heat-inactivated foetal bovine serum (CytoGen) and 1% (v/v) antibiotic–antimycotic solution (CytoGen), 1% (v/v) stable glutamine (L-alanyl-L-glutamine) solution (CytoGen), 1% (v/v) MEM non-essential amino acid solution (Sigma-Aldrich, St. Louis, MO, USA), and 1 mM sodium pyruvate (Sigma-Aldrich).

Cell lines were cultured at 37°C in a humidified atmosphere of 5% CO_2 in air. All experiments were performed in exponentially growing cultures. The compounds studied were added to the cultures as solutions in dimethyl sulfoxide (DMSO) (Sigma-Aldrich); control cultures were treated with the same volume of the solvent. The final concentration of DMSO

was maintained ca. 0.1%. After culturing the cells with the studied compounds for 24 or 48 h, the cells were collected and used for labelling.

2.3. Cell viability (MTT - colorimetric assay)

Cell viability was assessed using 3-(4,5-dimethylthiazol-2-yl)-2,5-diphenyltetrazolium bromide (MTT) (Sigma-Aldrich). All cells were cultured in 96-well plates with the addition of compounds and incubated for 48 h. MTT stock solution was added to each well to a final concentration of 0.5 mg/ml. After 4 h of incubation at 37°C, formazan crystals were dissolved by the addition of SDS-HCl solution (10% SDS in 0.001 M HCl, final concentration). MTT and SDS were added directly to the cell culture. The solubilized formazan product was spectrophotometrically quantified in a Power Wave XS (Bio Tek, Winooski, VT, USA) microplate reader at a wavelength of 570 nm. The MTT data were analysed to determine the IC_{50} values (concentration required to reduce the viability of cells by 50% compared with the control cells) of each compound. Regression analysis was performed with SigmaPlot software (San Jose, CA, USA).

2.4. Apoptosis assay by annexin V/propidium iodide (PI) labelling

Apoptosis was measured using the FITC Annexin V Apoptosis Detection Kit I (BD Pharmingen). After a 24- or 48-hour incubation with the tested agents, the cells were collected by centrifugation, rinsed twice with cold phosphate-buffered saline (PBS) and suspended in binding buffer at 1×10^6 cells/ml. Then, 100-µl aliquots of the cell suspension were labelled according to the kit manufacturer's instructions. Briefly, annexin V-FITC and PI were added to the cell suspension, and the mixture was vortexed and incubated for 15 min at room temperature in the dark. Then, 400 µl of cold binding buffer was added, and the cells were

vortexed again and kept on ice. Flow cytometry measurements were performed within 1 h after labelling.

2.5. Mitochondrial membrane potential ($\Delta\Psi_m$) assay

Mitochondrial membrane potential was assessed by flow cytometry using JC-1 (5,5',6,6'-tetrachloro-1,1',3,3'-tetraethylbenzimidazolocarbocyanine iodide; Sigma). JC-1 undergoes potential-dependent accumulation in mitochondria. In healthy cells, the dye accumulates in mitochondria, forming aggregates with red fluorescence (FL-2 channel), whereas in dead and apoptotic cells, the dye remains in the cytoplasm in a monomeric form and emits green fluorescence (FL-1 channel). Cells were harvested by centrifugation 48 h post-treatment, suspended in 1 ml of complete culture medium at approximately 1×10^6 cells/ml and incubated with 2.5 µl of JC-1 solution in DMSO (1 mg/ml) for 15 min at 37°C in the dark. The stained cells were then washed with cold PBS, suspended in 400 µl of PBS and then examined by flow cytometry.

2.6. Caspase activity

Active caspases in apoptotic cells were detected using Fluorescent Labelled Inhibitors of CAspases (FLICA) that covalently bind with active caspase enzymes. FLICA measures the intracellular process of apoptosis. If an active caspase enzyme is inside the cell, it will covalently bind with FLICA and retain the green fluorescent signal within the cell. Since non-apoptotic cells lack active caspases, these cells quickly return to their non-fluorescent status after the wash step. The activity of caspases was measured using the FAM-FLICA™ in vitro Caspase Detection Kit (ImmunoChemistry Technologies, LLC. MN, USA) applicable to flow cytometry. To detect specific caspases, cells were labelled by adding FLICA caspase-8 inhibitor reagent FAM-LETD-FMK (ImmunoChemistry Technologies, LLC.) or FLICA

caspase-9 inhibitor reagent FAM-LEHD-FMK (ImmunoChemistry Technologies, LLC.) according to the kit manufacturer's instructions. The cells were then washed twice and analysed directly on a flow cytometer.

2.7. Morphological evaluation (fluorescence and inverted microscopy)

After exposure to inhibitors, the cells were collected, washed with cold PBS and fixed with 70% ethanol at -20°C for at least 24 h. Next, ethanol was washed out, and the cells were stained with 1.0 μg/ml DAPI and 20 μg/ml sulforhodamine 101. Then, cell morphology was evaluated using a BX60 fluorescence microscope equipped with a DP50 digital camera (Olympus, Japan). Cell morphology was evaluated also using an ITM-2 inverted microscope equipped with a DP10 digital camera (Olympus, Japan).

2.8. Western blot analyses

The cells were washed with cold PBS buffer, and then, whole cell extractions were prepared using M-PER reagent (Pierce, Rockford, IL, USA). Protein concentration in the samples was measured using a BCA protein assay kit (Pierce). Equal amounts of proteins were loaded on 10% or 12% SDS-PAGE. After electrophoresis the proteins were transferred to a nitrocellulose membrane and probed with primary anti-human antibodies specific to: BAD, BCL-2, XIAP (Apoptosis I Sampler Kit) (BD Biosciences), PARP (113 kDa) (Apoptosis II Sampler Kit) (BD Biosciences), PARP (89 kDa) (BD Biosciences), phospho-Akt1 (Ser129) (Cell Signaling Technology), phospho-Bad (Ser112) (Cell Signaling Technology). Secondary antibodies conjugated with HRP were used. Protein bands were visualized using a CN/DAB substrate kit (Pierce) or Pierce™ 1-Step Ultra TMB-Blotting Solution (Pierce) or were detected by chemiluminescence on a MicroChemi (Bio-Imaging Systems).

2.9. Cell cycle analysis

After exposure to the tested compounds, the cells were washed with cold PBS and fixed at - 20 ºC in 70% ethanol for at least 24 h. Next, the cells were washed in PBS and stained with 50 μg/ml PI and 100 μg/ml RNase solution in PBST (PBS supplemented with 0.1% v/v Triton X-100) by 30 min incubation in the dark at room temperature. Cell DNA content and the distribution of the cells in different phases of the cell cycle were determined by flow cytometry employing CellQuest, BD FACSDiva software packages and MacCycle (Phoenix Flow Systems, San Diego, CA, USA).

2.10. Flow cytometry

Flow cytometry analyses were run on a FACSCalibur or FACSCanto II flow cytometer (BD Biosciences, San Jose CA, USA) and analysed using CellQuest, BD FACSDiva and WinMDI 2.9 software. The DNA histograms obtained were analysed using MacCycle software.

3. Results

3.1. Cytotoxic activity

Cytotoxic activity was determined for a series of deoxynucleosides carrying various tetrahalobenzimidazoles as aglycone moiety (see Fig. 1) by assessing the number of viable cells (KG-1, K562, LNCaP, PC-3) with the MTT assay. The MTT data were analysed to calculate the IC_{50} value of each compound. The results are given in Table 1. The studied inhibitors [K156, K157, K163, K164 (TDB) and K165] expressed IC_{50} values in the concentration range from 4.01 μM to 60.09 μM. Tetrabromo- (K164) and tetraiododerivatives (K165) appeared to be most cytotoxic, whereas a tetrachloroderivative (K156) exhibited rather low cytotoxicity. Compound K170 (dichloroderivative) appeared to be quite nontoxic (IC_{50} value >200 μM). The IC_{50} values of the most cytotoxic compound (K164) in cell lines

KG-1 and K562 were 4.01 μM and 8.51 μM, respectively (as compared to K165 where the respective values were 20.12 μM and 10.69 μM). K562 cells exhibited greater sensitivity to all tested compounds (except K164) compared to the KG-1 cell line. Among prostate cancer cell lines, LNCaP showed high sensitivity to the tested compounds, whereas PC-3 cells are resistant (Table 1).

3.2. Induction of apoptosis

Induction of apoptosis was assessed using Annexin V (FITC)/PI labelling after 24 and 48 h treatment of cells with the tested compounds. The studied inhibitors, used in the concentration range from 10 to 50 μM, evoked various proapoptotic effects in the leukaemia and prostate cell lines (Fig. 2). The observed apoptotic effects were time-dependent (K562, KG-1). Among the tested compounds, the most effective apoptosis inducers were again tetrabromo- (K164) and tetraiododerivatives (K165). On the other hand, compound K170 (dichloroderivative) exhibits no proapoptotic activity on any of the tested cell lines. Induction of apoptosis was highest in the LNCaP cell line. The percentage of apoptotic cells was 91.80 after 48 h exposure with 10 μM K164. Surprisingly, there is a lack of response from the PC-3 cells to any of the studied compounds, especially compared to another prostate cell line (LNCaP cell line) (Fig. 2). However, it should be noted that LNCaP cells responded to the compounds that were most active in cytotoxicity tests, tetrabromo- (K164) and tetraiododerivatives (K165), regardless of the dose but in a time-dependent manner (Fig. 2).

3.3. Mitochondrial membrane potential (ΔΨm)

Incubation with compound K164 and all remaining inhibitors (data not shown) caused mitochondrial membrane depolarization (as evidenced by the shift from red-to-green fluorescence ratio) in the KG-1, K562, LNCaP and PC-3 cell lines. This effect was dose-

dependent and may be linked to the intrinsic apoptotic pathway. Representative cytograms for the tetrabromoderivative (K164) and leukaemia as well as prostate cell lines are shown in Fig. 3.

3.4. Activity of caspases

The FLICA method was used to assess and identify apoptosis based on the detection of caspase activation in cell lines treated with compound K164 for 48 h. We found that in the process of apoptosis both caspase-8 and -9 are involved (Fig. 4).

3.5. Morphological changes in cells

The influence of compounds on the morphology of cells was observed by fluorescence microscope and inverted light microscope. No changes were observed for control cells. Characteristic apoptotic changes in the morphology of treated cells (changes in chromatin concentration and apoptotic body formation) were observed by fluorescence microscope, and changes in confluence of adherent cells were also observed. The morphology of cell lines treated with K164 is shown in Fig. 5.

3.6. Effect of compounds on the levels of proteins

To determine the levels of proteins important for the apoptosis process and two proteins, Akt1 and Bad, that are directly phosphorylated by protein kinase CK2 (Akt1) and PIM1 (Bad), we performed Western blot analysis of whole-cell extracts obtained from cells cultured in the presence of the most promising inhibitor K164 (concentration 10 μM, 20 μM, 50 μM) after 48 h of incubation. We found that levels of pro-apoptotic (Bad) and anti-apoptotic (BCL-2, XIAP) proteins decreased after treatment with K164 in KG-1, K562 and LNCaP cells with the exception of prostate cancer line PC-3. Interestingly, protein BCL-2 was not detected in

extracts obtained from K562 cells. Western blots tests showed that compound K164 at 20 μM and 50 μM induces PARP cleavage in the KG-1, K562 and LNCaP cell lines but no changes in the level of this protein in PC-3 cells. PARP cleavage (89 kDa) was dose-dependent. We can see that with the increase in the level of PARP (89 kDa), we observe a decrease in the level of PARP (113 kDa) in the KG-1 and K562 cell lines. The difference is in the case of LNCaP cells where the levels of both PARPs (89 kDA and 113 kDa) increased. Interestingly, there is a very high level of PARP (113 kDa) after treatment of LNCaP cells with K164 at a concentration of 20 μM and 50 μM, in line with its proapoptotic activity decrease. There was also a decrease in phosphorylated Akt1 (Ser129) and Bad (Ser112) protein levels in cell lysates obtained after treatment of cells (KG-1, K562, LNCaP) with the test compound. However, in KG-1 cells, the result is ambiguous in the case of phospho-Akt1 (Ser129) protein levels. An exemplary plot of Western blot analysis for K164 is presented in Fig. 6.

3.7. Effect of compounds on cell-cycle progression

Exemplary DNA histograms shown in Figure 7 demonstrate changes in cell-cycle progression of cells after 48 h of incubation with the most cytotoxic compound K164. This compound at concentrations of 20 μM and 50 μM induced large changes and perturbations in the cell cycle distribution; precise statistical analysis of the DNA histograms by the MacCycle computer programme was often impossible. Accumulation of cells in sub-G1 indicates of DNA degradation often seen in apoptotic cells. The compound K164 causes a concentration-depend accumulation of PC-3 cells in the G_2M phase and the border of S and G_2M phases, reducing the percentage of cells in G_1 phase of the cell cycle.

4. Discussion

In this paper, we have shown potential anticancer activity of selective inhibitors of protein kinases CK2 and PIM-1 on neoplastic cell lines. Compounds K156, K157, K163, K164 and K165 exhibited moderate to high cytotoxic and pro-apoptotic activity in KG-1 and K562 myeloid and LNCaP (but not PC-3) prostate cell lines (compound K170 was ineffective in all cell lines) (Table 1, Fig. 2). Among the compounds studied, K164 (1-(β-D-2′-deoxyribofuranosyl)-4,5,6,7-tetrabromo-1*H*-benzimidazole) appears to be the most promising. According to the previous publication, K164 inhibits CK2 by two mechanisms: an ATP site-directed mechanism and an allosteric one. K164 is purely competitive with respect to ATP (*Ki* = 0.015 μM) and to PIM-1 (*Ki* = 0.040 μM). To assess the selectivity of K164, this compound has been profiled at 1 μM concentration on a panel of 124 kinases. Only CLK2 and DYRK1A are inhibited by K164 as drastically as CK2 and PIM-1. K164 reduces towards the two protein kinases (IC_{50} = 0.032 μM with CK2 and 0.086 μM with PIM-1) (Cozza et al. 2014). Previous studies have also shown the cytotoxic efficiency of K164 with DC_{50} (concentrations inducing 50% cell death) values from 2.45±0.84 μM to 28.91±3.74 μM on different cell lines (Cozza et al. 2014).

These data encouraged us to pursue broader research on the series of inhibitors on neoplastic myeloid and prostate cell lines. We found that the most active compound K164 evoked high cytotoxic and pro-apoptotic effects in K562, a Philadelphia (Ph) chromosome-positive (BCR-ABL-positive) leukaemia cell line derived from chronic myeloid leukaemia (CML) in blast crisis (Lozzio et al. 1975) as well as in the BCR-ABL negative acute myelogenous leukaemia cell line KG-1. Compounds K156, K157, K163 and K165 exhibited higher cytotoxic and pro-apoptotic activity in the K562 cell line (as compared to KG-1 cell line). The results of investigations by Meeker et al. showed that among 37 human cell lines tested, the myeloid cell lines with highest expression of the *PIM-1* gene are K562 and KG-1 (Meeker et al. 1987,

1990). Moreover, kinase CK2 is highly expressed in proliferating myeloblastic cells from patients with acute myelogenous leukaemia (AML) or chronic myelogenous leukaemia (CML) in blastic crisis (Phan-Dinh-Tuy et al. 1985). The better efficiency of compounds in the K562 cell line could be explained in terms of a key role of PIM1 and CK2 kinases in the BCR/ABL-mediated cell protection from apoptosis. It should be noted that PIM1 can promote proliferation of BCR/ABL-transformed cells, inhibit activation of caspase-3 and stimulate cell cycle progression (Nieborowska-Skorska et al. 2002). CK2 is an essential mediator of BCR-ABL oncogenic signals. The BCR-ABL/CK2 complex is indeed responsible for mediating BCR-ABL induced cellular proliferation and survival. It was demonstrated that BCR-ABL is able to physically interact with CK2 in the K562 cell line via the ABL portion of the chimeric protein (Morotti et al. 2015).

In our study, we have shown that most of the tested inhibitors evoke cytotoxic and pro-apoptotic effects in two myeloid cell lines and one prostate cell line (Table 1, Fig. 2). An increase of mitochondrial permeability, cleavage of caspases-8 and -9 and characteristic changes in the morphology of cells accompanied their apoptosis process (Fig. 3-5).

These results may suggest intrinsic and extrinsic pathways of apoptosis induced by the dual inhibitors of CK2 and PIM-1. Unfortunately, compound K170 [1-(β-D-2′-deoxyribofuranosyl)-5,6-dichloro-1*H*-benzimidazole] does not exhibit cytotoxicity or proapoptotic activity on any of the cell lines tested (Table 1, Fig. 2), which may be due to its high IC_{50} value (>40 μM) for both CK2 and PIM-1 kinases (Cozza et al. 2014).

Additionally, the lack of response of PC-3 cells to all studied compounds in comparison to prostate cell line LNCaP should be noted (Fig. 2). This result may be related to the characteristics of the cell lines, for example PC-3 is an androgen-independent cell line that was derived from an advanced prostate carcinoma and expresses null p53, while LNCaP is an androgen-responsive human prostate adenocarcinoma derived from an early stage of prostate

carcinoma and expresses wild-type p53. It was found that the status of p53 is associated with the differential sensitivity observed in prostate cancer cells in response to treatment (Liu et al. 2013). On the other hand, other studies have shown that p53 is not required for the induction of apoptosis (Schneider et al. 2010).

Kinase CK2 plays a specific role in the proliferation regulation mechanism of prostate cancer. It has been shown that alterations in CK2 activity are dependent on the androgenic status were due to a rapid shutting of CK2 from chromatin structures into the nucleus and to the nuclear matrix. Moreover, it has been shown that androgen withdrawal in rats was followed by a rapid loss of CK2 from nuclear compartments and induced apoptosis. The increased responsiveness of androgen-sensitive cells compared with androgen-insensitive cells may relate to the observation that androgen receptor-mediated transcriptional activity is modulated by CK2. These data indicated tissue-specific signalling by CK2 (Wang et al. 2008; Ahmed et al. 2015).

In our study, we observed a decrease in pro-apoptotic activity of compound K164 in LNCaP cells at 20 μM concentration compared to 10 μM (Fig. 2). Based on our results it could be suggested that the above fact has an association with strong expression of the Poly(ADP-ribose) polymerase (PARP), which participates in DNA repair (Fig. 6).

We can see not only high levels of PARP protein (113 kDa) but also increased levels of PARP cleavage (89 kDa), proteins characteristic of apoptosis (Fig. 6). Western blot analysis of whole-cell extracts obtained from KG-1 and K562 cells cultured in the presence of K164 showed increased levels of PARP (89 kDa) and decreased levels of PARP (113 kDa). We discovered decreased levels of pro-apoptotic protein Bad (total) and phospho-Bad (Ser112) (Fig. 6). PIM-1 kinase promotes inactivation of the Bad protein by phosphorylating it on the Ser112 gatekeeper site and is one of several mechanisms via which the PIM-1 kinase can enhance BCL-2 activity and promote cell survival (Aho et al. 2005). Moreover, the level of phospho-AKT1 (Ser129) protein is decreased by the K164 inhibitor (Fig. 6). We have also

shown high levels of the anti-apoptotic proteins BCL-2 and X-linked inhibitor of apoptosis protein (XIAP) in PC-3 cell extracts (Fig. 6), which may affect resistance to apoptosis. Whereas our results also showed decreases in the levels of BCL-2 and XIAP in extracts obtained from cell lines (KG-1, LNCaP cells) after the treatment of cells with K164. The change in XIAP protein level in LNCaP cells seems to be very interesting. There is observed the very low level of this protein at 10 μM K164 compared to concentration of 20 μM and 50 μM. Protein BCL-2 was not detected in K562 cells in contrast to other cell lines. As shown in previous studies, K562 cells have high levels of BCL-xL without expression of BCL-2 (Benito et al. 1996; Yin et al. 2011). XIAP is a member of the inhibitors of apoptosis family of proteins (IAPs), and it is regulated by kinase CK2. Downregulation of CK2 results in loss of cellular IAPs in a distinct manner, and overexpression of CK2 protects IAPs from such downregulation induced by apoptotic signals (Wang et al. 2008).

In conclusion, our results showed that the majority of the tested inhibitors exhibited cytotoxic properties and induced apoptotic death in myeloid leukaemia and androgen-responsive prostate cell lines. The pro-apoptotic effects of the tested inhibitors may be related to the intrinsic and extrinsic pathway of apoptosis. Among all examined compounds, 1-(β-D-2′-deoxyribofuranosyl)-4,5,6,7-tetrabromo-1*H*-benzimidazole (K164) appears most promising for anticancer treatment, whereas its 5,6-dichloroanalogue is completely inactive.

Acknowledgements

This research was partly supported by the Foundation of Development of Diagnosis and Therapy (Warsaw, Poland).

References

Ahmed, K.A., Wang, G., Unger, G., Slaton, J., Ahmed, K., 2008. Protein kinase CK2 - A key suppressor of apoptosis. Advavces in Enzyme Regulation. (48), 179-87. https://dx.doi.org/10.1016%2Fj.advenzreg.2008.04.002.

Ahmed, K., Issinger, O.G., Szyszka, R., 2015. Protein Kinase CK2 Cellular Function in Normal and Disease States. (eds.). Springer. 111.

Aho, T.L., Sandholm, J., Peltola, K.J., Mankonen, H.P., Lilly, M., Koskinen, P.J., 2004. Pim-1 kinase promotes inactivation of the pro-apoptotic Bad protein by phosphorylating it on the Ser112 gatekeeper site. FEBS Lett. 571 (1-3), 43-49. https://10.1016/j.febslet.2004.06.050.

Amaravadi, R., Thompson, C.B., 2005. The survival kinases Akt and Pim as potential pharmacological targets. J. Clin. Invest. 115 (10), 2618–2624. https://dx.doi.org/10.1172%2FJCI26273

Benito, A., Silva, M., Grillot, D., Nuñez, G., Fernández-Luna, J.L., 1996. Apoptosis induced by erythroid differentiation of human leukemia cell lines is inhibited by Bcl-XL. Blood. (87), 3837-3843.

Brault, L., Gasser, C., Bracher, F., Huber, K., Knapp, S., Schwaller, J., 2010. PIM serine/threonine kinases in the pathogenesis and therapy of hematologic malignancies and solid cancers. Haematologica 95 (6), 1004–1015. https://dx.doi.org/10.3324%2Fhaematol.2009.017079.

Bretner, M., Najda-Bernatowicz, A., Łebska, M., Muszyńska, G., Kilanowicz, A., Sapota, A., 2008. New inhibitors of protein kinase CK2, analogues of benzimidazole and benzotriazole. Mol Cell Biochem. 316 (1), 87-89. http://link.springer.com/article/10.1007%2Fs11010-008-9827-0.

Cervantes-Gomez, .F, Chen, L.S., Orlowski, R.Z., Gandhi, V., 2013. Biological Effects of the Pim Kinase Inhibitor, SGI-1776, in Multiple Myeloma, Clinical Lymphoma, Myeloma & Leukemia 13 (2), 317-329. http://dx.doi.org/10.1016%2Fj.clml.2013.05.019.

Chen, L.S., Redkar, S., Bearss, D., Wierda, W.G., Gandhi, V., 2009. Pim kinase inhibitor, SGI-1776, induces apoptosis in chronic lymphocytic leukemia cells. Blood. 114 (19) 4150-4157. https://dx.doi.org/10.1182%2Fblood-2009-03-212852.

Cibull, T.L., Jones, T.D., Li, L., Eble, J.N., Ann Baldridge L., Malot,t S.R., Luo, Y., Cheng, L. 2006. Overexpression of Pim-1 during progression of prostatic adenocarcinoma. J Clin Pathol. 59 (3), 285-288. https://dx.doi.org/10.1136%2Fjcp.2005.027672.

Cozza, G., Sarno, S., Ruzzene, M., Girardi, C., Orzeszko, A., Kazimierczuk, Z., Zagotto, G., Bonaiuto, E., Di Paolo, M.L., Pinna, L.A., 2013. Exploiting the repertoire of CK2 inhibitors to target DYRK and PIM kinases. Biochim Biophys Acta 1834 (7), 1402–1409. https://dx.doi.org/10.1016/j.bbapap.2013.01.018.

Cozza, G., Girardi, C., Ranchio, A., Lolli, G., Sarno, S., Orzeszko, A., Kazimierczuk, Z., Battistutta, R., Ruzzene, M., Pinna, L.A., 2014. Cell-permeable dual inhibitors of protein kinases CK2 and PIM-1: structural features and pharmacological potential. Cell Mol Life Sci. 71 (16), 3173-3185. https://dx.doi.org/10.1007/s00018-013-1552-5

Dhanasekaran, S.M., Barrette, T.R., Ghosh, D., Shah, R., Varambally, S., Kurachi, K., Pient, K.J., Rubin, M.A., Chinnaiyan, A.M., 2001. Delineation of prognostic biomarkers in prostat cancer. Nature. 412, 822-826. https://dx.doi.org/10.1038/35090585.

Duncan, J.S., Litchfield, D.W., 2008. Too much of a good thing: the role of protein kinase CK2 in tumorigenesis and prospects for therapeutic inhibition of CK2. Biochim. Biophys. Acta 1784 (1), 33–47. https://dx.doi.org/10.1016/j.bbapap.2007.08.017.

Fedorov, O., Marsden, B., Pogacic, V., Rellos, P., Müller, S., Bullock, A.N,, Schwaller, J., Sundström, M., Knapp, S., 2007. A systematic interaction map of validated kinase inhibitors with Ser/Thr kinases. Proc Natl Acad Sci U S A 104 (51), 20523–20528. https://dx.doi.org/10.1073/pnas.0708800104.

Gianoncelli, A., Cozza, G., Orzeszko, A., Meggio, F., Kazimierczuk, Z., Pinna, L.A., 2009. Tetraiodobenzimidazoles are potent inhibitor of protein kinase CK2. Bioorg Med Chem 17 (20), 7281-7289. https://dx.doi.org/10.1016/j.bmc.2009.08.047.

Girardi, C., Ottaviani, D., Pinna, L.A., Ruzzene, M., 2015. Different Persistence of the Cellular Effects Promoted by Protein Kinase CK2 Inhibitors CX-4945 and TDB. Biomed Res Int. Article ID 185736, 9 pages. https://dx.doi.org/10.1155/2015/185736.

Holder, S., Zemskova, M., Zhang C, Tabrizizad, M., Bremer, R., Neidigh, J.W., Lilly, M.B., 2007. Characterization of a potent and selective small-molecule inhibitor of the PIM kinase. Mol Cancer Ther 6 (1), 163–172. https://dx.doi.org/10.1158/1535-7163.MCT-06-0397.

Janeczko, M., Orzeszko, A., Kazimierczuk, Z., Szyszka, R., Baier, A., 2012. CK2α and CK2α' subunits differ in their sensitivity to 4,5,6,7-tetrabromo- and 4,5,6,7-tetraiodo-1H-benzimidazole derivatives. European Jurnal of Medicinal Chemistry. 47 (1), 345-350. https://dx.doi.org/10.1016/j.ejmech.2011.11.002.

Kaminska, B., Ellert-Miklaszewska, A., Oberbek, A., Wisniewski, P., Kaza, B., Makowska, M., Bretner, M., Kazimierczuk, Z., 2009. Efficacy and mechanism of anti-tumor action of new potential CK2 inhibitors toward glioblastoma cells. Int J Oncol. 35 (5), 1091-100. DOI: 10.3892/ijo_00000424.

Kim, J.S., Eom, J.I., Cheong, J.W., Cho,i A.J,, Lee, J.K., Yang, W.I., Min, Y.H., 2007. Protein Kinase CK2α as an Unfavorable Prognostic Marker and Novel Therapeutic

Target in Acute Myeloid Leukemia. Clin. Cancer Res. 13 (3), 1019-1028. https://dx.doi.org/10.1158/1078-0432.CCR-06-1602.

Koronkiewicz, M., Żukowska, M., Chilmonczyk, Z., Orzeszko, A., Kazimierczuk, Z., 2010. Synthesis and proapoptotic properties if new casein kinase II inhibitors. Acta Pol Pharm 67 (6), 635-641. http://www.ptfarm.pl/pub/File/Acta_Poloniae/2010/6/635.pdf.

Koronkiewicz, M., Chilmonczyk, Z. Kazimierczuk, Z., 2013. Synergistic Anti-leukemic Effects of CK2 Inhibitors and Pentabromobenzylisothioureas In Vitro. Anticancer Res. 33 (11), 4891-4899. http://ar.iiarjournals.org/content/33/11/4891.full.pdf+html.

Kubiński, K., Masłyk, M., Orzeszko, A., 2017. Benzimidazole inhibitors of protein kinase CK2 potently inhibit the activity of atypical protein kinase Rio1. Mol Cell Biochem 426 (1-2), 195–203. https://dx.doi.org 10.1007/s11010-016-2892-x.

Laramas, M., Pasquie,r D., Filhol, O., Ringeisen, F., Descotes, J.L., Cochet, C., 2007. Nuclear localization of protein kinase CK2 catalytic subunit (CK2a) is associated with poor prognostic factors in human prostate cancer. Eur. J. Cancer 43 (5), 928-934. https://dx.doi.org/10.1016/j.ejca.2006.11.021.

Liu, C., Zhu, Y., Lou, W., Nadiminty, N., Chen, X., Zhou, Q., Shi, X.B., deVere White, R.W., Gao, A.C., 2013. Functional p53 determines docetaxel sensitivity in prostate cancer cells. Prostate. 73 (4), 418-427. https://dx.doi.org/10.1002/pros.22583.

Lopez-Ramos, M., Prudent, R., Moucadel, V., Sautel, C.F., Barette, C., Lafanechere, L., Mouawad, L., Grierson, D., Schmidt, F., Florent, J.C., Filippakopoulos, P., Bullock, A.N., Knapp, S., Reiser, J.B., Cochet, C., 2010. New potent dual inhibitors of CK2 and Pim kinases: discovery and structural insights. The FEBS Journal 24 (9), 3171-3185. https://dx.doi.org/10.1096/fj.09-143743.

Lozzio, C.B., Lozzio, B.B., 1975. Human chronic myelogenous leukemia cell-line with positive Philadelphia-chromosome. Blood 45 (3), 321–334. http://www.bloodjournal.org/content/bloodjournal/45/3/321.full.pdf.

Meeker, T.C., Nagarajan, L., ar-Rushdi, A., Rovera, G., Huebner, K., Croce, C.M., 1987. Characterization of the human PIM-1 gene: a putative proto-oncogene coding for a tissue specific member of the protein kinase family. Oncogene Res. 1 (1), 87-101.

Meeker, T.C., Loeb, J., Ayres, M., Sellers, W., 1990. The human Pim-1 gene is selectively transcribed in different hemato-lymphoid cell lines in spite of a G + C-rich housekeeping promoter. Mol Cell Biol. 10 (4), 1680-1688. https://www.ncbi.nlm.nih.gov/pmc/articles/PMC362273/pdf/molcellb00040-0390.pdf.

More, K.N., Jang, H.W., Hong, V.S., Lee, J., 2014. Pim kinase inhibitory and antiproliferative activity of a novel series of meridianin C derivatives. Bioorganic & Medicinal Chemistry Letters 24 (11), 2424-2428. https://dx.doi.org/10.1016/j.bmcl.2014.04.035.

Morotti, A., Carrà, G., Panuzzo, C., Crivellaro, S., Taulli, R., Guerrasio, A., Saglio, G., 2015. Protein Kinase CK2: A Targetable BCR-ABL Partner in Philadelphia Positive Leukemias. Adv Hematol. 2015, 612567. https://dx.doi.org/10.1155/2015/612567.

Nawijn, M.C., Alendar, A., Berns, A., 2011. For better or for worse: the role of Pim oncogenes in tumorigenesis. Nat. Rev. Cancer 11 (1), 23–34. https://dx.doi.org/10.1038/nrc2986.

Nieborowska-Skorska, M., Hoser, G., Kossev, P., Wasik, M.A., Skorski, T., 2002. Complementary functions of the antiapoptotic protein A1 and serine/threonine kinase pim-1 in the BCR/ABL-mediated leukemogenesis. Blood 99 (12), 4531-4539. http://www.bloodjournal.org/content/bloodjournal/99/12/4531.full.pdf.

O-charoenrat, P., Rusch, V., Talbot, S.G., Sarkaria, I., Viale, A., Socci, N., Nga, I,, Rao, P., d Singh, B., 2004. Casein Kinase II Alpha Subunit and C1-Inhibitor Are Independent

Predictors of Outcome in Patients with Squamous Cell Carcinoma of the Lung. Clin Cancer Res. 10 (17), 5792-803. https://dx.doi.org/10.1158/1078-0432.CCR-03-0317.

Pagano, M.A,, Meggio, F., Ruzzene,, M., Andrzejewska, M., Kazimierczuk, Z., Pinna, L.A., 2004. 2-Dimethylamino-4,5,6,7-tetrabromo-1H-benzimidazole: a novel powerful and selective inhibitor of protein kinase CK2. Biochem. Biophys. Res. Commun. 321 (4), 1040–1044. https://dx.doi.org/10.1016/j.bbrc.2004.07.067.

Pagano, M.A., Bain, J., Kazimierczuk, Z., Sarno, S., Ruzzene, M., Di Maira, G., Elliott, M., Orzeszko, A., Cozza, G., Meggio, F., Pinna, L.A., 2008. The selectivity of inhibitors of protein kinase CK2: an update. Biochem J. 415 (3), 353-365. https://dx.doi.org/10.1042/BJ20080309.

Phan-Dinh-Tuy, F., Henry, J., Boucheix, C., Perrot, J. Y., Rosenfeld, C., Kahn, A., 1985. Protein kinases in human leukemic cells. American Journal of Hematology 19 (3), 209–218. https://dx.doi.org/10.1002/ajh.2830190302.

Pinna, L.,A., 2012. Protein kinase CK2. Wiley, New York.

Pogacic, V., Bullock, A.N., Fedorov, O., Filippakopoulos, P., Gasser, C., Biondi, A., Meyer-Monard, S., Knapp, S., Schwaller, J., 2007. Structural analysis identifies imidazo[1,2-b]pyridazines as PIM kinase inhibitors with in vitro antileukemic activity. Cancer Res 67 (14), 6916–69124. https://dx.doi.org/10.1158/0008-5472.CAN-07-0320.

Reiser-Erkan, C.1., Erkan, M., Pan, Z., Bekasi, S., Giese, N.A., Streit, S., Michalski, C.W., Friess, H., Kleeff, J., 2008. Hypoxia-inducible proto-oncogene Pim-1 is a prognostic marker in pancreatic ductal adenocarcinoma. Cancer Biol Ther. 7 (9), 1352-1359.

Sarno, S., Reddy, H., Maggio, F., Ruzzene, M., Davies, S.P., Donella-dean, A., Shuger, D., Pinna, A., 2001. Selectivity of 4,5,6,7-tetrabromobenzotriazole, an ATP site-directed inhihitor of protein kinase CK2 (“casein kinase-2”). FEBS Lett 496: 44-48.

Schneider, C.C., Hessenauer, A., Montenarh, M., Götz, C., 2010. p53 is dispensable for the induction of apoptosis after inhibition of protein kinase CK2. The Prostate 70 (2), 126-134. https://dx.doi.org/10.1002/pros.21044.

Schneider, C.C., Kartarius, S., Montenarh, M., Orzeszko, A., Kazimierczuk, Z., 2012. Modified tetrahalogenated benzimidazoles with CK2 inhibitory activity are active against human prostate cancer cells LNCaP in vitro. Bioorganic & Medicinal Chemistry. 20 (14), 4390-4396. https://dx.doi.org/10.1016/j.bmc.2012.05.038.

Siddiqui-Jain, A., Drygin, D., Streiner, N., Chua, P., Pierre, F., O'Brien, S.E., Bliesath, J., Omori, M., Huser, N., Ho, C., Proffitt, Ch., Schwaebe, M.K., Ryckman, D.M., Rice, W.G., Anderes, K., 2010. CX-4945, an Orally Bioavailable Selective Inhibitor of Protein Kinase CK2, Inhibits Prosurvival and Angiogenic Signaling and Exhibits Antitumor Efficacy. Cancer Res 70 (24), 10288-10298. https://dx.doi.org/10.1158/0008-5472.CAN-10-1893.

Trembley, J.H., Chen, Z., Unger, G., Slaton, J., Kren, B.T., Van Waes, C., Ahmed, K., 2010. Emergence of Protein Kinase CK2 as a Key Target in Cancer Therapy. Biofactors. 36 (3), 187-195. https://dx.doi.org/10.1002/biof.96.

Wang, G., Ahmad, K.A., Harris, N.H., Ahmed, K., 2008. Impact of protein kinase CK2 on inhibitor of apoptosis proteins in prostate cancer cells. Mol Cell Biochem 316 (1-2), 91–97. https://dx.doi.org/10.1007/s11010-008-9810-9.

Yin, S., Wang, R., Zhou, F., Zhang, H., Jing, Y., 2011. Bcl-xL is a dominant antiapoptotic protein that inhibits homoharringtonine-induced apoptosis in leukemia cells. Mol Pharmacol. 79 (6), 1072-1083. https://doi.org/10.1124/mol.110.068528.

Zien, P., Bretner, M., Zastapilo, K., Szyszka, R., Shugar, D., 2003. Selectivity of 4,5,6,7-tetrabromobenzimidazole as an ATP-competitive potent inhibitor of protein kinase

CK2 from various sources. Biochem. Biophys. Res. Commun. 306 (1), 129–133. http://www.sciencedirect.com/science/article/pii/S0006291X03009288.

Figures and legend:

Fig. 1. Synthesis of 2'-deoxyribo-nucleosides of 4,5,6,7-tetrahalogeno- and 5,6-dichloro-benzimidazoles 1-6.

Fig. 2. Induction of apoptosis (sum of early and late apoptosis) by agents in KG-1, K562, LNCaP, and PC-3 cells. The data were determined by FACS cytometer after 24 and 48 h of treatment. Cells were stained with annexin V-FITC and PI. Each bar represents the mean ± S.D. ($n \geq 4$).

Fig. 3. Representative flow cytograms demonstrating changes in mitochondrial membrane potential ($\Delta\Psi m$) of all cells induced by 48 h of culturing with K164 compound. The cells were stained with JC-1 dye. The cells in the lower right region (R2) showed increased green fluorescence (apoptotic cells).

Fig. 4. Representative flow histograms demonstrating active caspases in KG-1 cells (panel A), K562 cells (panel B) , LNCaP cells (panel C) and PC-3 cells (panel D) treated with K164 (50 μM) compound for 48 h. Marker M1 designates the negative cell population whereas M2 designates the positive cell population indicating caspase activity. Cells were labelled by adding caspase-8 inhibitor reagent (FAM-LETD-FMK) or FLICA caspase-9 inhibitor reagent (FAM-LEHD-FMK).

Fig. 5. Morphology of cells cultured for 48 h. Panel A. Inverted microscopy (light observation, 100x magnification). Panel B. Fluorescence microscopy (400x magnification). Morphological examination of cells stained with DAPI/sulforhodamine 101. Cells were harvested, fixed and stained with DAPI for DNA (blue fluorescence) and sulforhodamine 101 for protein (red fluorescence). Arrows indicate apoptotic bodies (Panel B).

Fig. 6. Western blot analysis of B-cell lymphoma 2 (BCL-2) family proteins (pro- and anti-apoptotic), PARP proteins (panel A) and phosphorylated proteins (panel B) in whole cell extracts obtained from cell lines cultured in the presence of K164 (concentration 10 μM, 20 μM, 50 μM) after 48 h of incubation. Preparation of cell extracts and protein detection are described in Materials and Methods. All bands were quantified by densitometric analysis and their intensity normalized with respect to β-actin. The ratio of the studied proteins to β-actin for cell lines incubated in the absence of K164 was assumed to be 1.

Fig. 7. Exemplary DNA histograms of cell lines treated for 48 h with K164 compound (stained with propidium iodide). The data obtained from the flow cytometer were analysed using MacCycle software to determine the percentage of cells in each phase of the cell cycle.

Table 1. IC_{50} values of compounds studied (MTT - assay; $n \geq 3$).

	IC_{50} [μM]; 48h			
Compound	KG-1	K562	LNCaP	PC-3
K156	60.09 ± 12.16	45.06 ± 6.86	22.50 ± 0.13	> 50
K157	34.65 ± 4.98	12.51 ± 4.33	29.27 ± 5.96	> 50
K163	32.91 ± 5.73	23.65 ± 1.57	30.08 ± 5.36	> 50
K164	4.01 ± 0.70	8.51 ± 0.62	ND*	> 50
K165	20.12 ± 7.65	10.69 ± 3.63	8.23 ± 0.75	ND
K170	> 100	> 100	> 200	> 200

*Not Designated (cells respond regardless of the dose)

Fig. 1.

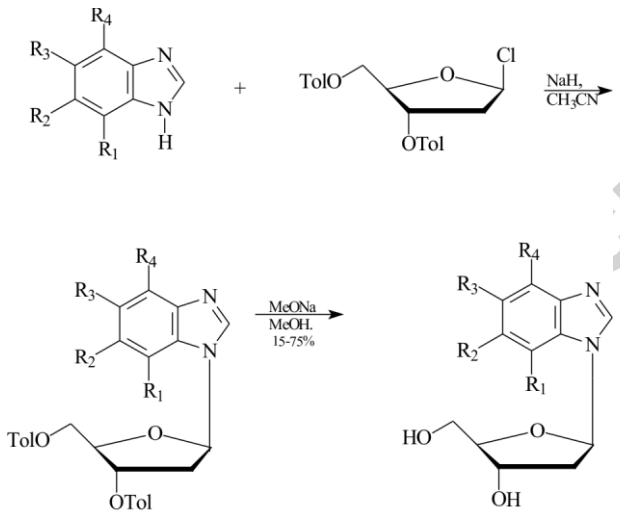

1-6

compound	R_1	R_2	R_3	R_4
1 (K156)	Cl	Cl	Cl	Cl
2 (K157)	I	Cl	Cl	I
3 (K163)	Br	Cl	Cl	Br
4 (K164)	Br	Br	Br	Br
5 (K165)	I	I	I	I
6 (K170)	H	Cl	Cl	H

Fig. 2.

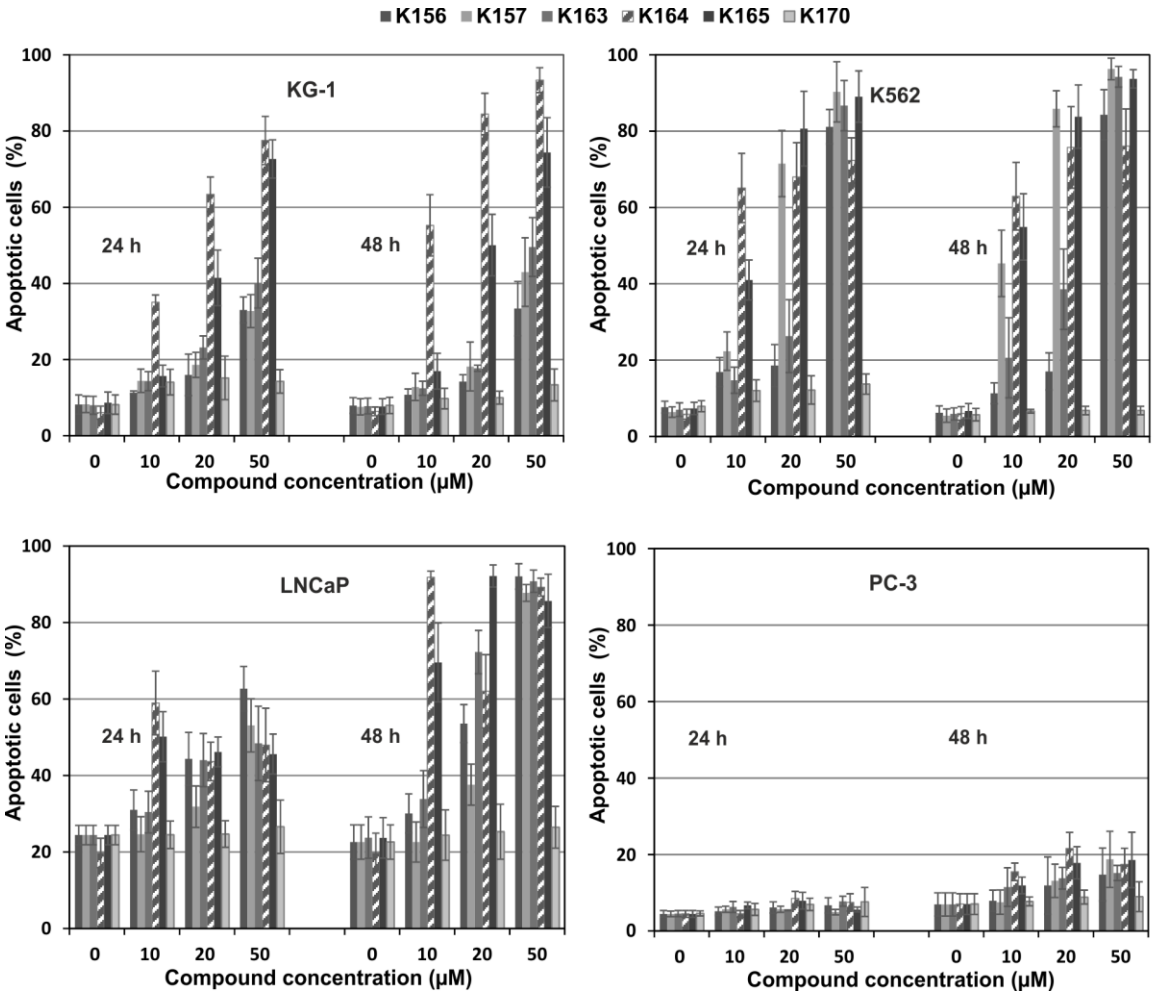
K156 K157 K163 K164 K165 K170
KG-1
K562
LNCaP
PC-3
24 h
48 h
Apoptotic cells (%)
Compound concentration (μM)
0 10 20 50 0 10 20 50
0 20 40 60 80 100

Fig. 3.

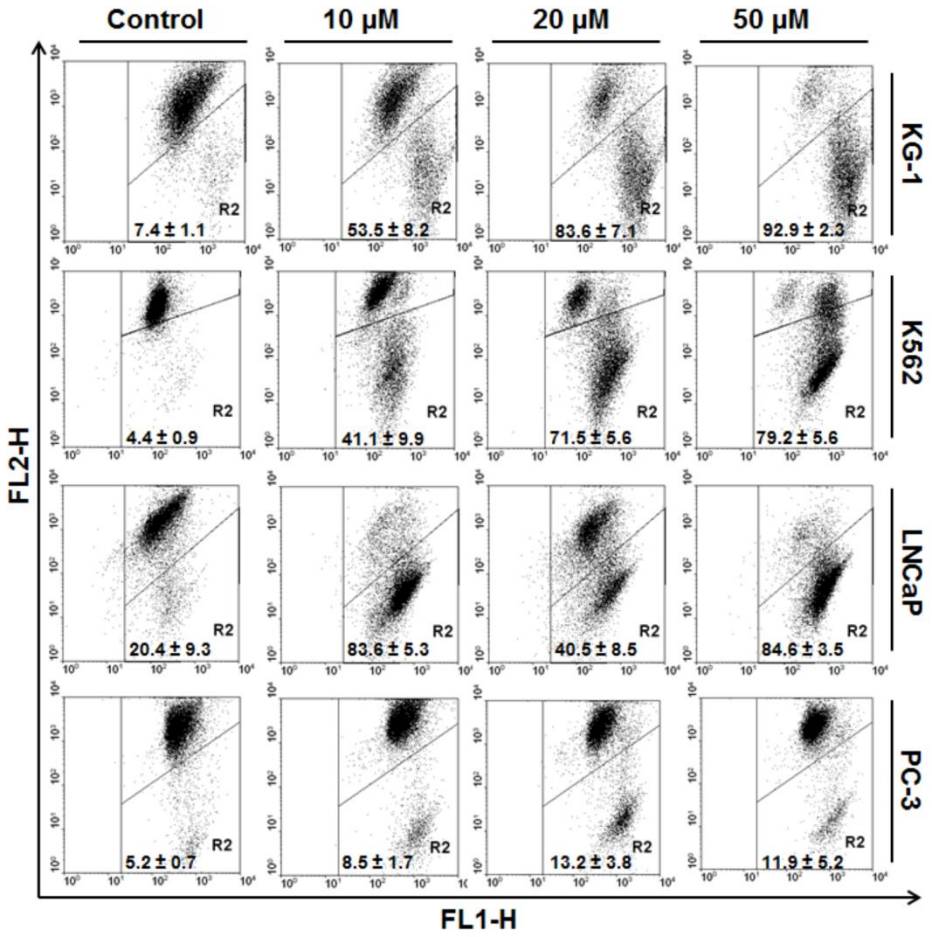
Control
10 μM
20 μM
50 μM
KG-1
K562
LNCaP
PC-3
R2
7.4 ± 1.1
53.5 ± 8.2
83.6 ± 7.1
92.9 ± 2.3
4.4 ± 0.9
41.1 ± 9.9
71.5 ± 5.6
79.2 ± 5.6
20.4 ± 9.3
83.6 ± 5.3
40.5 ± 8.5
84.6 ± 3.5
5.2 ± 0.7
8.5 ± 1.7
13.2 ± 3.8
11.9 ± 5.2
FL2-H
FL1-H

Fig. 4.

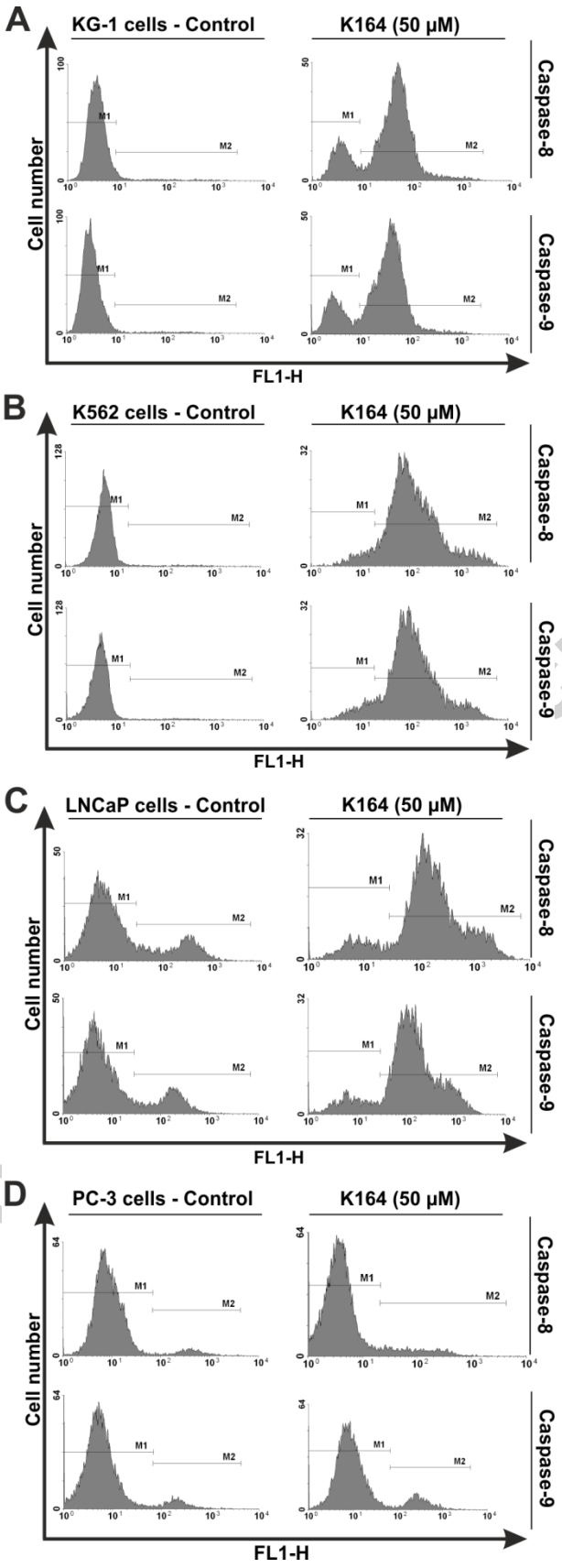
A
KG-1 cells - Control
K164 (50 μM)
Caspase-8
Caspase-9
Cell number
FL1-H
M1
M2
B
K562 cells - Control
K164 (50 μM)
Caspase-8
Caspase-9
Cell number
FL1-H
C
LNCaP cells - Control
K164 (50 μM)
Caspase-8
Caspase-9
Cell number
FL1-H
D
PC-3 cells - Control
K164 (50 μM)
Caspase-8
Caspase-9
Cell number
FL1-H

Fig. 5.

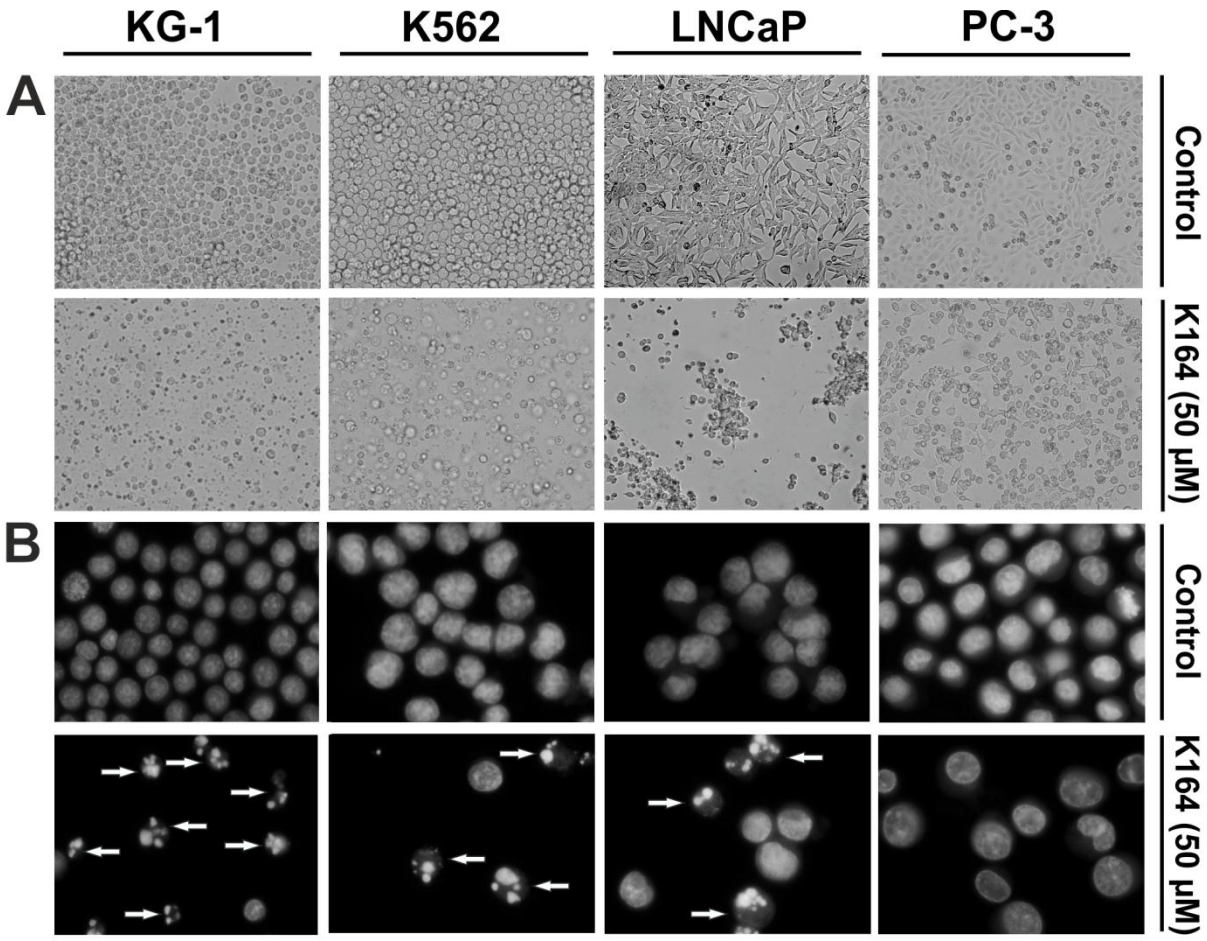

Fig. 6.

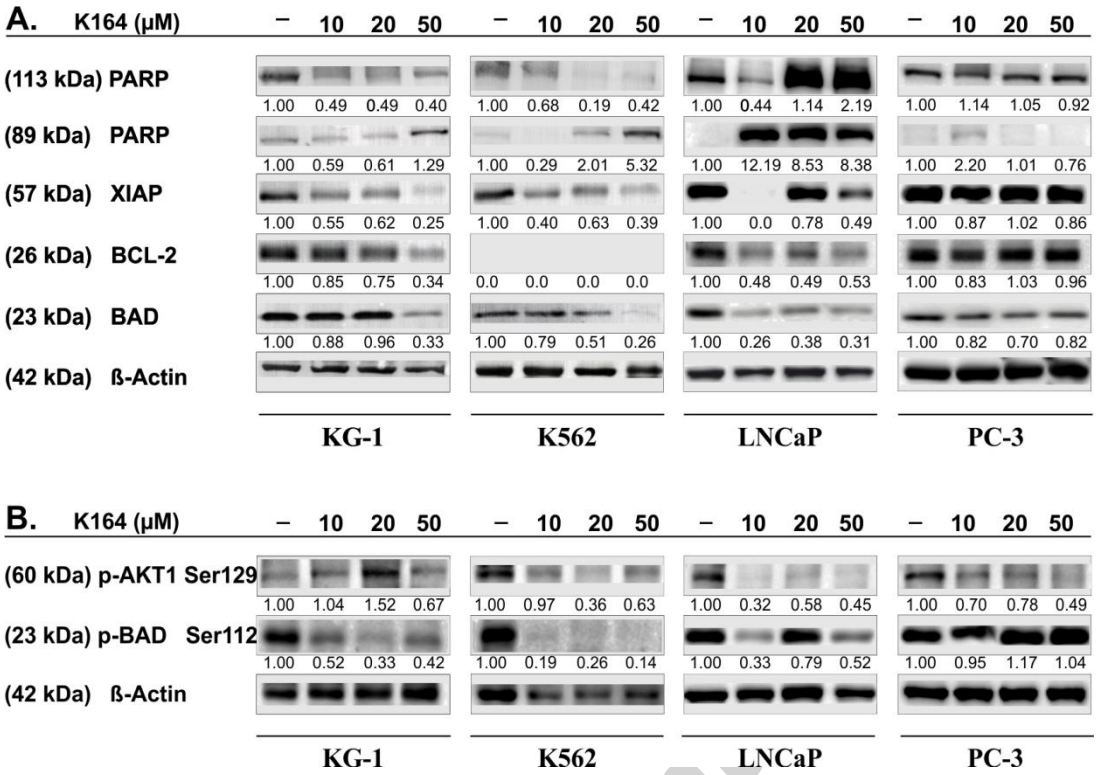

Fig. 7.

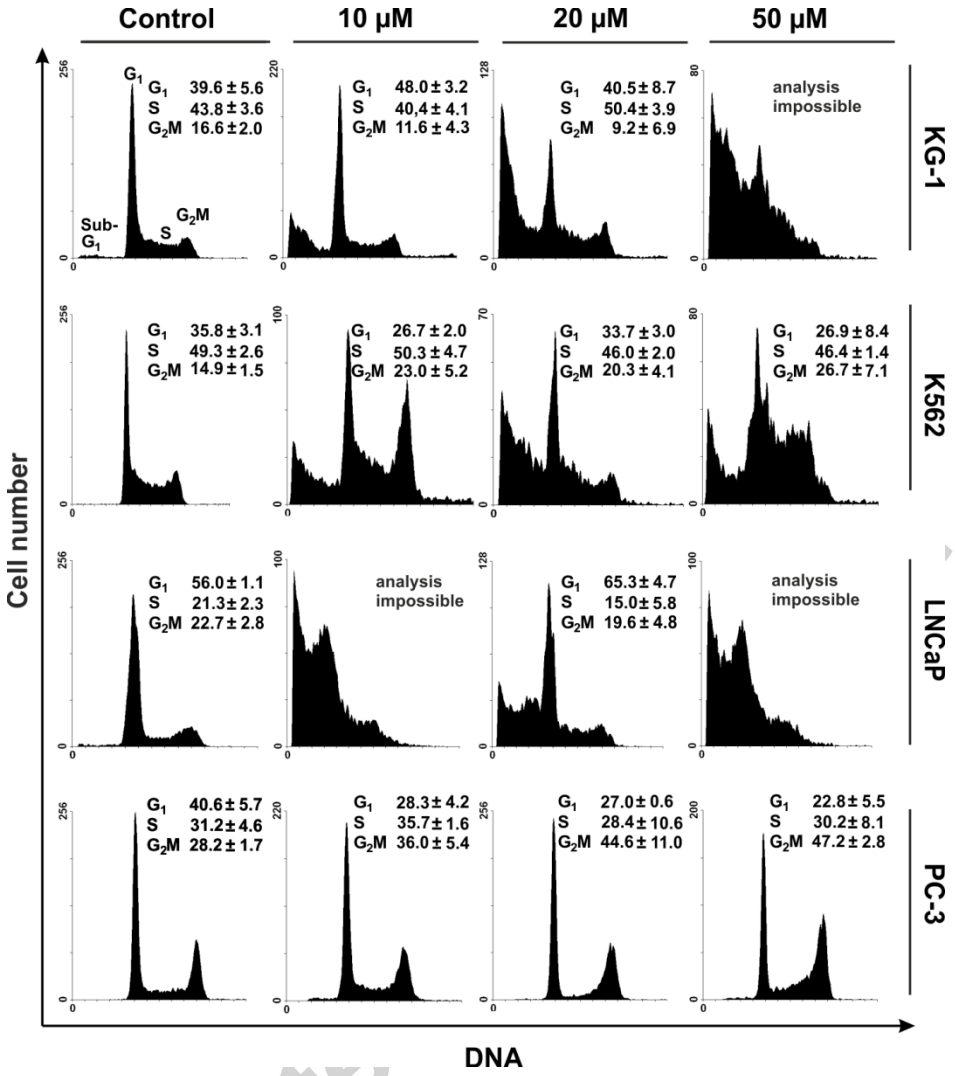
Control
10 μM
20 μM
50 μM
KG-1
K562
LNCaP
PC-3
Cell number
DNA
Sub-G1
G1
S
G2M
G1 39.6 ± 5.6
S 43.8 ± 3.6
G2M 16.6 ± 2.0
G1 48.0 ± 3.2
S 40,4 ± 4.1
G2M 11.6 ± 4.3
G1 40.5 ± 8.7
S 50.4 ± 3.9
G2M 9.2 ± 6.9
analysis impossible
G1 35.8 ± 3.1
S 49.3 ± 2.6
G2M 14.9 ± 1.5
G1 26.7 ± 2.0
S 50.3 ± 4.7
G2M 23.0 ± 5.2
G1 33.7 ± 3.0
S 46.0 ± 2.0
G2M 20.3 ± 4.1
G1 26.9 ± 8.4
S 46.4 ± 1.4
G2M 26.7 ± 7.1
G1 56.0 ± 1.1
S 21.3 ± 2.3
G2M 22.7 ± 2.8
analysis impossible
G1 65.3 ± 4.7
S 15.0 ± 5.8
G2M 19.6 ± 4.8
analysis impossible
G1 40.6 ± 5.7
S 31.2 ± 4.6
G2M 28.2 ± 1.7
G1 28.3 ± 4.2
S 35.7 ± 1.6
G2M 36.0 ± 5.4
G1 27.0 ± 0.6
S 28.4 ± 10.6
G2M 44.6 ± 11.0
G1 22.8 ± 5.5
S 30.2 ± 8.1
G2M 47.2 ± 2.8